Surface polarization effects in confined polyelectrolyte solutions

Debarshee Bagchi[a], Trung Dac Nguyen[b], and Monica Olvera de la Cruz[a,b,c,1]

[a]Department of Materials Science and Engineering, Northwestern University, Evanston, IL 60208; [b]Department of Chemical and Biological Engineering, Northwestern University, Evanston, IL 60208; and [c]Department of Physics and Astronomy, Northwestern University, Evanston, IL 60208

Contributed by Monica Olvera de la Cruz, June 24, 2020 (sent for review April 21, 2020; reviewed by Rene Messina and Jian Qin)

Understanding nanoscale interactions at the interface between two media with different dielectric constants is crucial for controlling many environmental and biological processes, and for improving the efficiency of energy storage devices. In this contributed paper, we show that polarization effects due to such dielectric mismatch remarkably influence the double-layer structure of a polyelectrolyte solution confined between two charged surfaces. Surprisingly, the electrostatic potential across the adsorbed polyelectrolyte double layer at the confining surface is found to decrease with increasing surface charge density, indicative of a negative differential capacitance. Furthermore, in the presence of polarization effects, the electrostatic energy stored in the double-layer structure is enhanced with an increase in the charge amplification, which is the absorption of ions on a like-charged surface. We also find that all of the important double-layer properties, such as charge amplification, energy storage, and differential capacitance, strongly depend on the polyelectrolyte backbone flexibility and the solvent quality. These interesting behaviors are attributed to the interplay between the conformational entropy of the confined polyelectrolytes, the Coulombic interaction between the charged species, and the repulsion from the surfaces with lower dielectric constant.

polyelectrolytes | confinement | dielectric mismatch | energy storage | negative differential capacitance

Polyelectrolytes under spatial confinement are of great interest to physical and life sciences (1, 2), as well as to modern technologies (3). In supercapacitors, also referred to as electrical double-layer capacitors, ionic liquids or electrolyte solutions are typically confined between two carbon-based electrodes like graphene. Supercapacitors can be competitive energy storage devices since they are cheaper, safer, and more environmentally friendly as compared to standard lithium–ion batteries. Currently, aqueous solutions of electrolytes are being investigated as supercapacitor materials, and impressive battery performance has been reported (4). In such confined systems, both simple and molecular electrolytes exhibit intriguing phenomena, such as charge inversion and overcharging (5), breakdown of local charge neutrality (6), enhanced repulsions (7) or attractions (8), enhanced mobility (9), and nonmonotonic electrophoretic mobility (10).

The physical properties of polyelectrolyte solutions in contact with charged surfaces are of practical and fundamental interest (1, 11, 12). In supercapacitors and batteries, the relative permittivity of the electrodes is typically very different from that of the solution. Such dielectric discontinuity results in a jump in the electric field at the interface, which manifests as surface polarization (13–15). However, most studies, to date, do not include surface polarization effects, based on the assumption that it would be negligible when the surfaces are charged. Studies on simple electrolytes taking into account only one dielectric discontinuity found that polarization effects are negligible, except when the surface is weakly charged (16) or when it is corrugated and the ions are multivalent (17). Electrolytes confined by metallic electrodes have been studied using constant potential boundary conditions (18, 19). However, for many biological settings as well as in supercapacitor applications, molecular electrolytes confined by dielectric materials, such as graphene, are of interest. Recent studies on dielectric confinement of polyelectrolyte by a spherical cavity showed that dielectric mismatch leads to unexpected symmetry-breaking conformations, as the surface charge density increases (20). The focus of the present study is the collective effects of spatial confinement by two parallel surfaces and dielectric mismatch on the structural features of a polyelectrolyte solution.

In order to explore and exploit the effect of confinement on polyelectrolyte solutions, we analyze surface polarization effects by varying the polyelectrolyte degree of flexibility, polyelectrolyte charge fraction, surface charge density, and dielectric contrast between the solution and the confining surfaces. We determine the highly debated effect of surface polarization on the physical properties of polyelectrolyte solutions, including the possibility and degree of charge amplification (5) and charge inversion (21), as the surface charge density increases, and, in the case of confinement by metallic electrodes, as a function of the imposed surface potential.

Another long-standing problem in the context of electrical double-layer capacitors is the issue of negative differential capacitance. By definition, the differential capacitance of a double layer characterizes the change in the charge storage with respect to the change in the voltage across the double layer. Equilibrium

Significance

Molecular electrolytes under confinement are crucial materials for energy storage devices and commonly used model systems for understanding biomolecular functions. In particular, understanding the complex interplay of entropy and electrostatic interactions in a polyelectrolyte solution confined inside oppositely charged surfaces gives us important insights into its energy storage and capacitance properties. Here, using molecular dynamics simulations, we analyze polyelectrolyte solutions confined between two oppositely charged planar surfaces with a much lower dielectric constant. We find that such mismatch of dielectric constants and chain flexibility significantly influence the energy storage capability and capacitance of such a confined system. Dielectric mismatch enhances surface charge amplification in flexible polyelectrolyte solutions, increasing their energy storage capabilities.

Author contributions: D.B., T.D.N., and M.O.d.l.C. designed research; D.B. and T.D.N. performed research; D.B., T.D.N., and M.O.d.l.C. analyzed data; and D.B., T.D.N., and M.O.d.l.C. wrote the paper.

Reviewers: R.M., University of Lorraine; and J.Q., Stanford University.

The authors declare no competing interest.

[1]To whom correspondence may be addressed. Email: m-olvera@northwestern.edu.

This article contains supporting information online at https://www.pnas.org/lookup/suppl/doi:10.1073/pnas.2007545117/-/DCSupplemental.

First published August 3, 2020.

thermodynamics and statistical mechanics (22, 23) suggest that the differential capacitance should always be strictly positive, but this conclusion was challenged by later works (24, 25). Attard et al. (24) pointed out that there exists no rigorous proof that the differential capacitance has to be positive for an isolated double layer. Simulations of $1:2$ electrolyte solutions also demonstrate that the differential capacitance can become negative (25). Similar results were reported for charge- and size-symmetric electrolytes, in the presence of a large spherical macroion, and the emergence of the negative differential capacitance was explained in terms of the compactness of the double layer (26). Moreover, subsequent studies (27, 28) suggest that, in a uniform charge density controlled system, the differential capacitance of one double layer can become negative, as long as the differential capacitance of both of the double layers taken together remains positive, whereas, when the electrodes are held at constant electrostatic potentials, the differential capacitance will always be positive.

Here, we show that dielectric mismatch between the polyelectrolyte solution and the confining walls exhibits nontrivial effects on the electrical double layers near the charged interfaces. We demonstrate that such effects lead to the negative differential capacitance of the double layer for a certain range of the surface charge density. Furthermore, we observe that polarization effects result in the noticeably enhanced energy storage in the electrical double layer, which can be useful for supercapacitor design.

The paper is organized as follows. We first study flexible polyelectrolytes for various surface charge densities, and then we investigate the roles of chain flexibility, solvent dielectric constant, and boundary conditions at the confining surfaces, in determining the capacitative behavior and energy storage of the double-layer structure.

Atomistic simulations typically allow investigation of small systems. In order to draw conclusions based on large systems and a broader range of system parameters, we use here an implicit solvent–explicit ions coarse-grained model of the confined polyelectrolyte system. Typical configurations of the polyelectrolyte solution are depicted in Fig. 1. Each polyelectrolyte is represented by a linear bead-spring chain with randomly placed charged beads (29). The charge fraction is defined as $f_q = n/N$, where n is the total number of charged monomer beads, each with one electron charge $-Ze$, and N is the total number of monomers. For overall electroneutrality, we have added n positive counterion beads with $+Ze$ charge. The polyelectrolytes and counterions are confined between two planar surfaces, each composed of spherical beads arranged into a square lattice. The positively charged surface is placed at $z = 0$, and the negatively charged surface is placed at $z = H$. Unless otherwise stated, we employ the fixed-charge boundary conditions, where each surface bead is assigned a partial charge such that the surface charge density is Σ. The confining surfaces are composed of a material of low dielectric constant, $\epsilon_1 = 2$. The solvent is

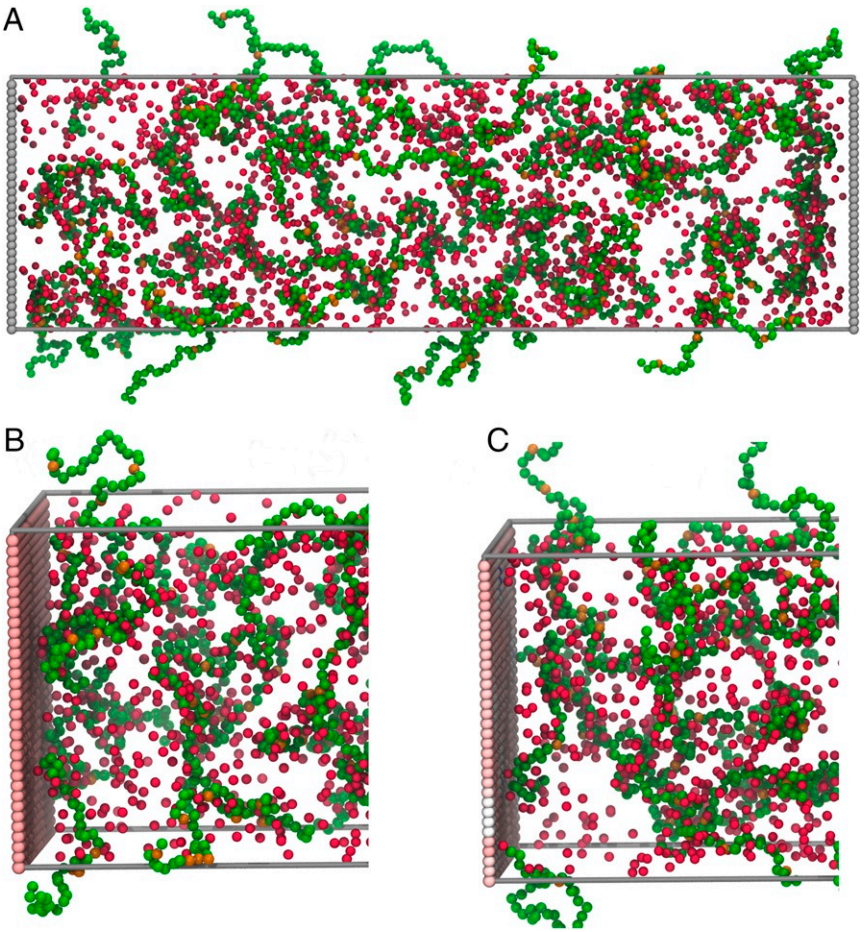

Fig. 1. Typical configurations of the polyelectrolyte solution confined between two dielectric planar surfaces, for polyelectrolyte charge fraction $f_q = 0.9$. The green, orange, and red beads represent charged monomers, neutral monomers, and counterions, respectively. The three snapshots correspond to (*A*) uncharged surfaces with polarization, (*B*) charged surface without polarization, and (*C*) charged surface with polarization. In *B* and *C*, the region near the positively charged surface is shown.

modeled as a continuum background with uniform dielectric constant $\epsilon_2 = 80$. To take into account the polarization due to dielectric mismatch between the surfaces and the solution, we solve for the induced charges at every molecular dynamics (MD) time step using the methods described in our recent work (30). Specific details of our model and simulation method are given in *Materials and Methods* and *SI Appendix*.

Results and Discussion

Charge Density Profiles. The structural features of the charged species in the electrical double layer are characterized by the time-averaged net charge density profiles $\rho(z) = \rho_+(z) - \rho_-(z)$, where ρ_+ and ρ_- are the charge densities of the positively charged counterions and the negatively charged monomers, respectively. We first plot $\rho(z)$ in Fig. 2*A*, for three different values of the charge fraction f_q, without polarization effects as the baseline. The negatively charged polyelectrolyte chains accumulate near the positively charged surface at $z = 0$, whereas the positively charged counterions accumulate near both of the surfaces. This can be seen from the typical configuration shown in Fig. 1*B* for polyelectrolyte charge fraction $f_q = 0.9$. This accumulation of counterions near a like-charged surface is referred to as *charge amplification* (also referred to as *overcharging*) (5, 21, 31), and becomes more pronounced for higher f_q values (Fig. 2*A*, *Inset*). This phenomenon arises because the gain in entropy of the counterions is larger than the repulsion they experience due to the like-charged surface. However, charge amplification is observed only for low surface charge densities Σ; for higher Σ values, the repulsion between the surface and the counterions becomes large, and charge amplification disappears. In Fig. 2*B*, we show $\rho(z)$ for an equivalent electrolyte solution, which is identical to the polyelectrolyte solution except that all of the bonds are removed. Unlike the polyelectrolyte system, however, the net charge density profile for the electrolyte solution does not show charge amplification. This suggests that charge amplification is due to the interplay between the gain in the configurational entropy of the counterions (mentioned earlier) and the penalty in conformational entropy of the polyelectrolytes adsorbed to the surface. As will be shown later, the difference in the charge density profiles translates into the difference in the Coulombic energy stored in the double layers between the two systems.

The cumulative charge density $\rho_c(z) = \int_0^z \rho(s)\,ds$ for the polyelectrolyte solution near both surfaces (Fig. 2*C*) is found to be larger in magnitude than the surface charge density Σ. Each surface attracts more charges of the opposite sign than what is necessary to neutralize its charge, which is a phenomenon known as *charge inversion* (21, 32). Note that charge amplification (the positive part of the curve in Fig. 2*C*) is observed only in the double layer near the positively charges surface, but charge inversion is observed near both surfaces. The polyelectrolyte solution exhibits charge inversion at the surfaces even if there is no charge amplification, while all of these effects are absent in the electrolyte system shown in Fig. 2*D*.

When polarization effects due to dielectric mismatch between the surface and the solution are taken into account, the charge distribution of the polyelectrolyte solution is altered in two aspects (Fig. 3*A*). First, the density profile is shifted away from the positively charged surface (as can be seen in Fig. 3*A*, *Inset*); that is, the polyelectrolyte solution experiences more confinement when polarization effects are present. Therefore, dielectric mismatch (when $\epsilon_1 < \epsilon_2$) effectively adds an extra confinement effect to the polyelectrolytes and counterions on top of the spatial confinement due to the impenetrable surfaces. Second, charge amplification becomes stronger in the presence of polarization effects, indicated by the increased peak heights h_+ near the positively charged surface, as can be seen in Fig. 3*B*, for different surface charge densities. Comparing Fig. 1 *B* and *C*, it can be seen that the polyelectrolyte chains are repelled away from the wall in the presence of polarization effects, and the space between the positively charged surface and the polyelectrolyte layer is occupied by more counterions.

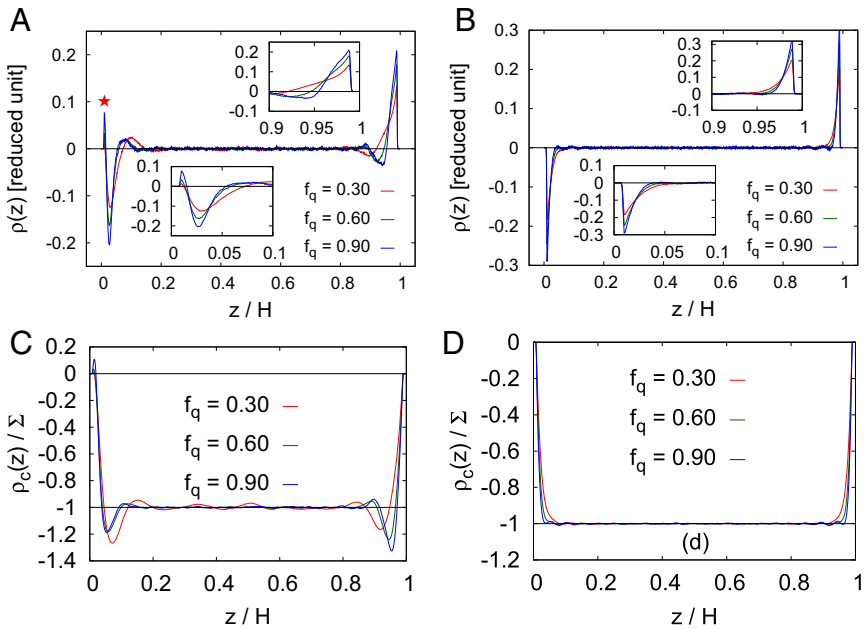

Fig. 2. (*A* and *B*) Net charge density profile $\rho(z)$ for different values of the charge fraction f_q for (*A*) polyelectrolyte solution and (*B*) electrolyte solution, with all parameters being the same. *Insets* magnify the density profile near the two surfaces. The red star in *A* shows the position of counterion accumulation near the positively charged surface that leads to charge amplification. (*C* and *D*) Cumulative charge density $\rho_c(z)$ scaled by the interface charge density Σ for different values of the charge fraction f_q for (*C*) polyelectrolyte solution and (*D*) electrolyte solution, computed from the data in *A* and *B*, respectively. The surface charge density is $\Sigma = 0.04$ C·m^{-2}.

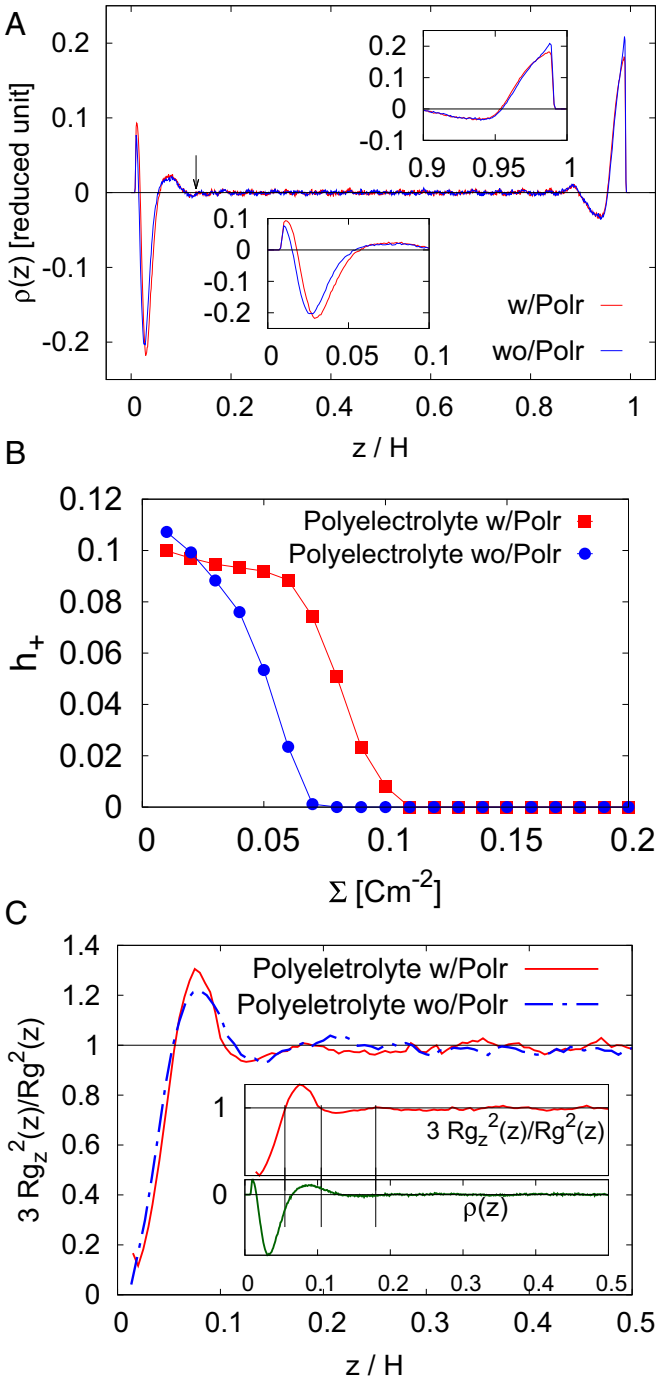

Fig. 3. (*A*) Comparison of the charge density profile $\rho(z)$ of the polyelectrolyte solution for $f_q = 0.90$ with (w/Polr) and without (wo/Polr) polarization effects for surface charge density $\Sigma = 0.04$ C·m^{-2}. The region between the positively charged surface and the point marked by the arrow is considered as the double layer. *Insets* magnify the charge density profile near the charged surfaces. (*B*) The height of the charge amplification peak for different values of the surface charge density Σ, with and without polarization. (*C*) The normalized radius of gyration of the polyelectrolytes $3R^2_{gz}(z)/R^2_g$ with and without polarization for $f_q = 0.40$. In *Inset*, $3R^2_{gz}(z)/R^2_g$ is shown against the net charge density $\rho(z)$ for the polyelectrolyte solution with polarization effects.

Interesting features in the conformation of the polyelectrolyte chains are observed in the double layer formed near the positively charged surfaces. The average squared radius of gyration is defined as $R^2_g = \langle(\vec{r}_i - \vec{r}_{cm})^2\rangle$ and its components $R^2_{g\alpha} = \langle(\vec{r}^{\,\alpha}_i - \vec{r}^{\,\alpha}_{cm})^2\rangle$, where $\alpha \equiv x, y, z$; $\langle\cdot\rangle$ denotes the average over all of the polyelectrolyte chains. As can be seen from Fig. 3*C*, in the bulk, $3R^2_{gz}(z)/R^2_g \approx 1$, and the chains, on average, have a spherically symmetric conformation. However, next to the positively charged surface $3R^2_{gz}(z)/R^2_g < 1$, the polyelectrolyte chains are compressed along the $z-$ direction into an oblate spheroid conformation. Thereafter, $3R^2_{gz}(z)/R^2_g > 1$ overshoots the bulk value. In the overshoot region, the chains are more elongated along the z direction and assume a prolate spheroid conformation. The flipping from a z-compressed oblate to a z-elongated prolate conformation occurs in a region that mostly has a net positive charge, that is, with excess counterions (Fig. 3*C*, *Inset*). The oblate–prolate flipping happens more than once, indicating that the polyelectrolyte chains arrange themselves in alternate layers of z-compressed and z-elongated conformations under confinement. The conformational flipping therefore can be attributed to the polyelectrolyte chains trying to minimize the electrostatic repulsion of the neighboring layers of polyelectrolyte chains. The overshooting peak is more prominent in the presence of polarization, where the confinement effects are stronger. This phenomenon is reminiscent of the *cubatic* phase that was observed originally in simulation studies of hard cut spheres (33), although the scenario is much more complicated here.

We note that, for confining surfaces that have a higher dielectric constant than the solution (i.e., $\epsilon_1 > \epsilon_2$), the charges are attracted toward the surfaces in the presence of polarization effects, even when the surface charge density is zero. The charge density near the surfaces exhibits higher peaks near the surface compared to the case where there is no dielectric mismatch, $\epsilon_1 = \epsilon_2$ (*SI Appendix*, Fig. S1).

Differential Capacitance and Energy Storage in the Double Layers. We first obtain the electrostatic potential profile $\Phi(z)$ between the two surfaces from the net charge density profile $\rho(z)$ by numerically integrating the Poisson's equation, $\partial^2_z\Phi(z) = -\rho(z)/(\epsilon_0\epsilon_2)$, where ϵ_2 is the solvent dielectric constant and ϵ_0 is the vacuum permittivity. The boundary conditions are chosen as $\Phi(z=0) = 0$ and $E(z = H/2) = -\partial_z\Phi(z = H/2) = 0$.

Typical potential profiles $\Phi(z)$ obtained from the simulations for the polyelectrolyte and an electrolyte solution (which is the same as the polyelectrolyte solution but with all of the bonds between the monomers removed) are shown in Fig. 4*A* (see also *SI Appendix*, Fig. S2). We denote the potential drop between the positively charged surface and the bulk as Φ_+ (and similarly for Φ_-) which is the voltage drop across the electric double layer (EDL) and is referred to as the EDL potential. Here the EDL is identified from the charge density profile, where $\rho(z)$ first approaches the bulk value from the positively charged surface (marked by an arrow in Fig. 3*A*). For the polyelectrolyte solution, $\Phi_+ \neq \Phi_-$, unlike for the electrolyte solution. Here, we will focus on the EDL potential Φ_+, since this is the voltage drop across the double layer formed near the positively charged surface where the polyelectrolyte chains get absorbed.

The differential capacitance of the double-layer structure, C_d, is defined as $C_d = (d\Phi_+/d\Sigma)^{-1}$, where the double-layer potential Φ_+ for different values of the surface charge density Σ is shown in Fig. 4*B*. When polarization effects are neglected, Φ_+ increases monotonically with increasing Σ, similar to what is observed with electrolyte solutions. When polarization effects are included, however, the relationship between Φ_+ and Σ becomes nonmonotonic. Specifically, for $\Sigma < 0.1$ C·m^{-2}, Φ_+ increases with increasing Σ. In this regime, the difference in Φ_+ with and without polarization effects is due to the increase in the charge amplification peak h_+ in the presence of polarization effects (Fig. 3*B*).

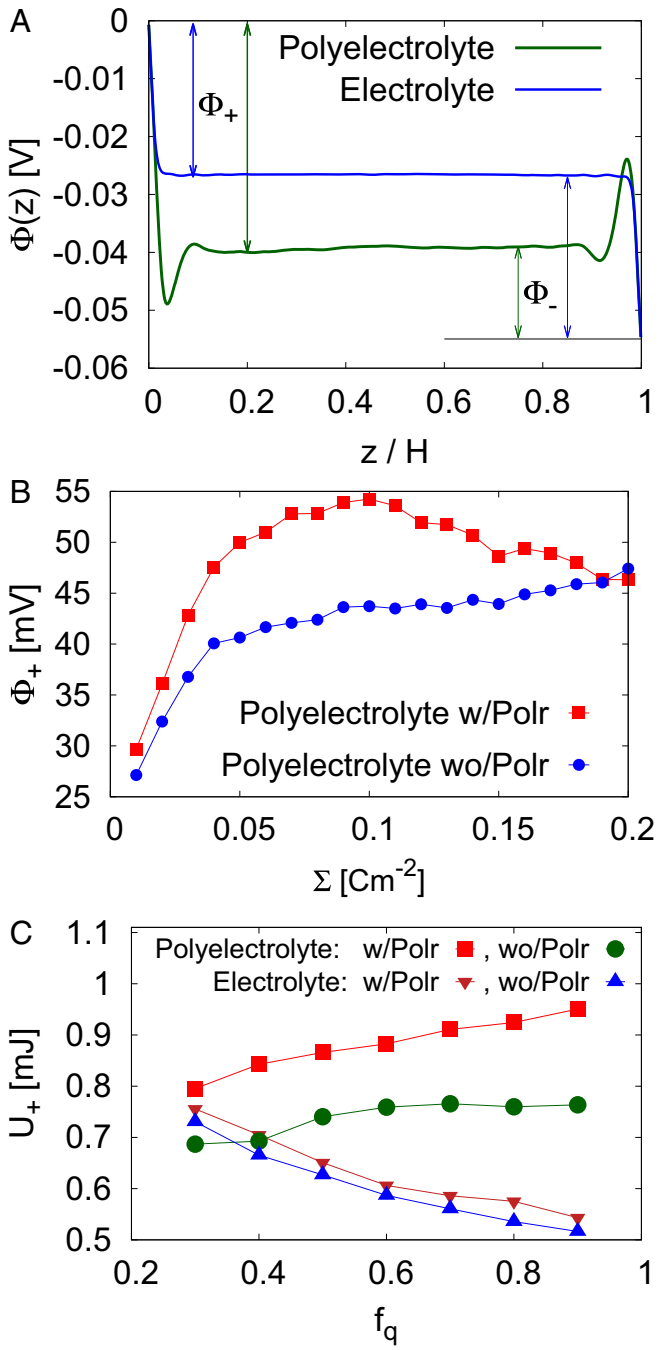

Fig. 4. (*A*) Electrostatic potential profiles $\Phi(z)$ of the polyelectrolyte and electrolyte solutions for charge fraction $f_q = 0.90$. The arrows show how the potential drops from the charged surfaces to the bulk are determined. (*B*) The variation of the EDL potential Φ_+ for different values of surface charge density Σ with (filled squares) and without (filled circles) polarization effects. (*C*) The double-layer electrostatic energy U_+ with charge fraction f_q for the electrolyte solution and the polyelectrolyte solution, with and without polarization effects. The surface charge density is $\Sigma = 0.04$ C·m^{-2} in *A* and *C*.

For $0.1 \le \Sigma \le 0.2$ C·m^{-2}, we observe a negative differential capacitance, $C_d < 0$, as Φ_+ decreases from 55 mV to 45 mV with increasing Σ. In this regime, charge amplification at the positively charged surface vanishes, as indicated by h_+ being zero (Fig. 3*B*). This means that the Coulombic attraction between the negatively charged polyelectrolytes and the positively charged surface is sufficiently strong to deplete all of the counterions from the surfaces. The spatial distribution of the net charge density of the EDL in the *x*–*y* plane reveals that the charges are heterogeneously distributed (*SI Appendix*, Figs. S3 and S4). For the given range of Σ, the in-plane charge densities have a broader distribution around the mean value compared to the case where polarization effects are excluded (*SI Appendix*, Fig. S5).

For greater values of surface charge density, $\Sigma > 0.2$ C·m^{-2}, the polyelectrolyte–surface Coulombic attraction dominates, and Φ_+ always increases with Σ regardless of whether or not polarization effects are included (*SI Appendix*, Fig. S6*A*). The emergence of the EDL negative differential capacitance within a certain range of Σ seems to result from a complex interplay between excluded volume correlations, polyelectrolyte conformational entropy, and electrostatic interactions between the charges in the EDL and with the confining surfaces.

Note that the total potential drop $\Phi = \Phi_+ + \Phi_-$ always increases monotonically for all value of Σ (*SI Appendix*, Fig. S6*B*); that is, the total capacitance remains positive. This is indeed consistent with the suggestion by Partenskii et al. (27) and Partenskii and Jordan (28). We find that differential capacitance is always positive for 1:1 and 1:3 electrolyte solutions (*SI Appendix*, Fig. S7). The nonmonotonic behavior of the electrostatic potential with the surface charge density without polarization was previously reported for electrolyte solution surrounding a spherical macroion (26). The difference between those and our findings in confined electrolytes is due to the size and shape of the confining surfaces (planar versus spherical) and the parameter regimes explored.

A crucial point that we want to make here is regarding the importance of polarization effects and its dependence on surface charge density Σ (Fig. 4*B*). Although the general belief is that polarization effects become increasingly unimportant as Σ increases (see ref. 34 and references therein), Fig. 4*B* demonstrates that this is not true for the electrostatic potential. Let us define $\Delta\Phi_+ = |\Phi_+^p - \Phi_+^0|/(\Phi_+^p + \Phi_+^0)$ as an indicator of the importance of polarization effects, where Φ_+^p and Φ_+^0 are the values with and without polarization, respectively. We find that $\Delta\Phi_+$ reaches the maximum value around $\Sigma_* = 0.07$ C·m^{-2} for the particular system under investigation. As a result, the effect of polarizability on the electrostatic potential drop Φ_+ across the EDL is most prominent in the vicinity of Σ_* and is small on either side of this Σ_* value. We expect that both Σ_* and the range over which polarization effects are important would be a function of various parameters such as chain flexibility and solvent dielectric constant, as shown below.

The electrostatic energy stored in the EDL (per unit surface area L^2) is given by $U_+ = 1/2\Phi_+ Q_+/L^2$, where Q_+ is obtained from numerically integrating the net charge density profile $\rho(z)$ inside the EDL. We plot the energy storage U_+ as a function of the polyelectrolyte charge fraction f_q for a fixed surface charge density $\Sigma = 0.04$ C·m^{-2} in Fig. 4*C*. The energy storage in the polyelectrolyte EDL is higher than the energy stored in the electrolyte EDL. Moreover, the energy stored for the polyelectrolyte solution is further enhanced when one takes into account the effects of polarization. Also, the effects of polarization for the polyelectrolyte solution are appreciably stronger than those in the electrolyte solution. This suggests that it is more favorable to choose polyelectrolytes over electrolytes for energy storage devices.

From the supercapacitor design point of view, it is of practical importance to understand the capacitative and energy storage behaviors of the double-layer structure as functions of key design parameters such as chain flexibility, solvent dielectric constant, and boundary conditions at the surfaces. We will discuss the effects of these factors in the following sections.

Chain Flexibility. To represent the flexibility (or stiffness) of the polyelectrolytes, we constrain the angles between the

adjacent bonds along the polyelectrolyte backbone with a harmonic potential $U(\theta) = K_\theta(\theta - \theta_0)^2$, where the stiffness constant $K_\theta = 100\epsilon$, and equilibrium angle $\theta_0 = 180°$. Here, θ is the angle between two adjacent bond vectors $\mathbf{r}_{i,i-1}$ and $\mathbf{r}_{i,i+1}$, where $\mathbf{r}_{i,j}$ is the vector pointing from monomer i to monomer j. The effects of the backbone rigidity in the emergence of the negative differential capacitance can be realized by comparing the EDL potential for the stiffer chains (Fig. 5*A*, red squares) with that for the fully flexible chains (shown in Fig. 4*B*, red squares). For any given value of Σ, the EDL potential for the stiffer chains is smaller than for the fully flexible chains. Also, the negative differential capacitance is observed over a larger range $0.04 < \Sigma < 0.16$ C·m^{-2}, where Φ_+ decreases from 40 mV to 15 mV. Notably, for stiffer polyelectrolyte chains, we find, from Fig. 5*A*, that negative differential capacitance emerges even in the absence of polarization effects for $0.04 < \Sigma < 0.12$ C·m^{-2}. Recall that, for the fully flexible chains (i.e., $K_\theta = 0$), C_d is always positive without polarization effects, suggesting that the reduced conformational entropy of the stiffer chains is another factor that leads to the negative slope and nonmonotonic behavior of the Φ_+ versus Σ curve.

The net charge density profiles (*SI Appendix*, Fig. S8) further reveal that the EDL formed by the rigid polyelectrolytes is more compact than the fully flexible polyelectrolyte EDL. This is presumably because the rigid chains have a lower conformational entropy, and therefore can form a more compact double layer near the surface. Moreover, charge amplification is also found to be more pronounced in the case of rigid polyelectrolytes. These results suggest that the higher double-layer compactness and charge amplification are strongly related to the more pronounced negative differential capacitance that is observed for rigid polyelectrolytes.

Regarding the Coulombic energy stored in the EDL, we find that, while U_+ for the fully flexible chains increases roughly linearly with the surface charge density Σ, it appears to be nonmonotonic for the stiffer chains (Fig. 5*B*), which is correlated with the variation of Φ_+. Moreover, U_+ for the stiffer chains is considerably smaller than for the fully flexible chains. This is because the number of the (positively charged) counterions in the EDL for the stiffer chains is smaller than that for the fully flexible counterparts, or, in other words, the number of counterions released to the bulk is greater for the stiffer chains.

Solvent Dielectric Constant. For a solvent with a lower dielectric constant $\epsilon_2 = 40$ (e.g., ethylene glycol), the electrostatic interactions are twice as strong as in water. As can be seen in Fig. 6*A*, the nonmonotonic relationship between Φ_+ and Σ persists in the presence of polarization effects. In fact, the region of negative differential capacitance, for $\epsilon_2 = 40$, begins at a lower value of the surface charge density $\Sigma \approx 0.05$ C·m^{-2} as compared to $\Sigma \approx 0.1$ C·m^{-2} for $\epsilon_2 = 80$. This is attributed to a more compact EDL that is formed in the lower dielectric constant solvent, because of the stronger electrostatic interactions between the charged monomers and the confinement surface. We also find that, as Σ increases, the solvent with a higher dielectric constant stores more electrostatic energy in the polyelectrolyte EDL, as shown in Fig. 6*B*.

Constant Potential Boundary Conditions. We study a limiting case of surface polarization where ϵ_1 approaches infinity; that is, we consider the surfaces (electrodes) to be metallic, as in batteries. In this limit, the electrical field inside each electrode vanishes, and the electrostatic potential at the electrode surface is constant. Under the applied electrostatic potential difference between the electrodes, $\Delta\Phi$, the electrode charge fluctuations can be sampled from Boltzmann statistics (23). Although there are numerous approaches for handling the constant potential boundary conditions in MD simulations (18, 19, 35–37), here we follow the method proposed by Petersen et al. (19) for computational efficiency. For our simulations, we approximate the metallic materials by setting the dielectric constant of the electrodes to be $\epsilon_1 = 5{,}000$ and computing the contributions from the primary and higher-order image charges to the fluctuating electrode charges using the energy functional approach (30, 38).

For small potential differences $\Delta\Phi$, charge amplification is present at the positive electrode similar to what is observed with carbon-based electrodes (Fig. 2*A*). However, a negative differential capacitance was not observed; that is, the charge stored in the polyelectrolyte EDL always increases monotonically with Φ_+ (*SI Appendix*, Fig. S9) for all of the different constant potential differences studied. This validates the claim, mentioned earlier, that negative differential capacitance emerges only in the uniform charge density ensemble, but not in the constant potential ensemble, where differential capacitance plays a role similar to susceptibility (23, 27). Thus, the result obtained from the uniform charge density ensemble is inequivalent to the constant potential ensemble. This is reminiscent of the specific heat in systems with long-ranged interactions: The specific heat can become negative in the microcanonical ensemble, but is always positive in the canonical ensemble, thus giving rise to ensemble inequivalence in long-ranged interacting systems (39). Although the two boundary conditions, fixed charge density and constant potential, may yield different differential capacitance behaviors, they are not completely unrelated: A negative differential capacitance in the uniform charge density boundary conditions implies interfacial instabilities and phase transitions in a constant potential controlled system (27). Note that negative differential capacitance was also predicted to occur in a third kind of thermodynamic constraint where the total charge on the confining surfaces is held constant and the local charge density is fluctuating (27).

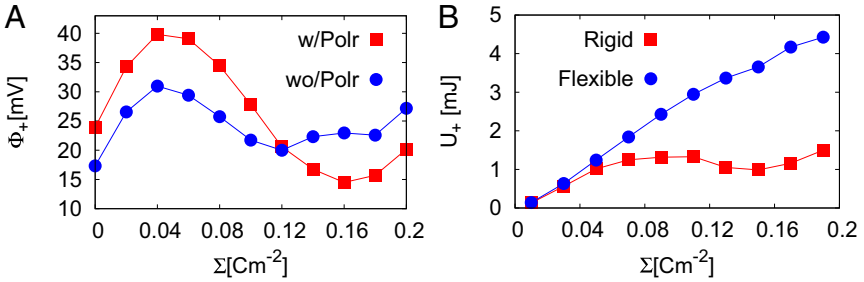

Fig. 5. (*A*) Comparison of the EDL potential Φ_+ for a solution of stiff polyelectrolytes, in the presence and absence of polarization effects. (*B*) Comparison of energy storage U_+ in the double layer near the positively charged surface for the rigid and the fully flexible polyelectrolyte solutions, in the presence of polarization effects.

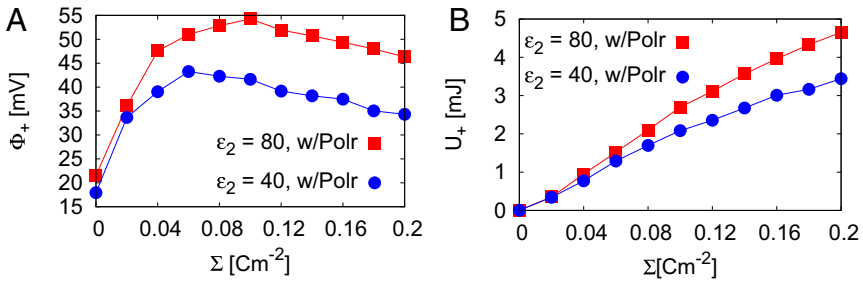

Fig. 6. (*A*) Comparison of the EDL potential Φ_+ for a polyelectrolyte solution with solvent dielectric constants $\epsilon_2 = 80$ and 40, in the presence of polarization effects. (*B*) Comparison of energy storage U_+ in the double layer near the positively charged surface for the two cases.

Polyelectrolytes in a Good Solvent. All of the simulation results presented so far are performed under poor solvent conditions where the nonbonded non-Coulombic interaction between the monomers is represented by the Lennard-Jones (LJ) interaction. To investigate the effect of a good solvent, we switch to using the purely repulsive Weeks–Chandler–Andersen potential for the nonbonded interaction between the monomers. We find that charge amplification in a good solvent is weaker when compared to that in poor solvents (*SI Appendix*, Fig. S10). This is because, unlike in a poor solvent, the polyelectrolyte chains in a good solvent are more stretched out and can approach the confining surface more closely, thus leaving less space near the surface that can be occupied by the counterions. Due to this weaker charge amplification, energy storage in the polyelectrolyte double layer is lower under good solvent conditions when compared to poor solvents. The effect of polarization in a good solvent is the same as in poor solvents: It enhances polyelectrolyte double-layer energy storage (*SI Appendix*, Fig. S10*D*).

Conclusion

We conclude our discussion with a few remarks. First, compared to electrolyte solutions, polyelectrolyte solutions under confinement exhibit a much richer behavior with more tunable parameters, and the ability to store more electrostatic energy. Second, polarization effects due to dielectric mismatch lead to enhanced charge amplification, emergence or enhancement of negative differential capacitance, and increased energy storage in the EDL for a certain range of surface charge density. This implies that polarization effects for charged surfaces have a considerable effect on the charge distribution inside the confinement, and thus cannot be neglected. Finally, our simulations indicate that all of the crucial double-layer properties, such as charge amplification, energy storage, and differential capacitance, are strongly dependent on the conformational entropy of the polyelectrolyte chains, that, in turn, depends on chain flexibility, the quality of the solvent, and the solvent dielectric constant. In particular, energy storage is found to be higher for flexible polyelectrolytes in a poor solvent with a larger dielectric constant and in the presence of surface polarization effects. Thus, the nontrivial effects due to dielectric mismatch reported in this study suggest that polarization effects should be included accurately at interfaces and in heterogeneous charged systems in general.

Materials and Methods

We use the linear bead-spring model to represent the polyelectrolyte chains, each composed of $N_p = 40$ beads, and there are 60 chains in a typical simulation. Counterions are added to the system to ensure overall charge neutrality. The nonbonded interaction between the particles is modeled by the standard 12–6 LJ potential with the cutoff distance of $r_c = 2.5\sigma$, where σ is the length scale of the LJ potential. The particle charge Z is chosen such that the Bjerrum length in the solution $l_B = (Ze)^2/(4\pi\epsilon_0\epsilon_2 k_B T)$ = 0.7 nm. The Coulombic interaction is computed using the particle–particle particle mesh method with an accuracy of 10^{-4}. The bonded interaction between the monomers is modeled by the finitely extensible nonlinear elastic springs with the spring constant of $k = 30\epsilon/\sigma$ and $R_0 = 1.5\sigma$, where ϵ is the LJ well depth. The dimensionless temperature is defined as $T^* = k_B T/\epsilon$ and set to be 1.0 throughout our simulations. The dimensionless time unit is defined as $\tau = \sigma\sqrt{m/\epsilon}$, where m is the particle mass being identical for all of the monomers and counterions. The distance between the two substrates is fixed at $H = 100\sigma$. When polarization effects are taken into account, we compute the induced charges for each substrate particle at every time step using the methods described in ref. 30. All of the simulations were performed with Large-Scale Atomic/Molecular Massively Parallel Simulator (LAMMPS) version 16 July 2018. More details on our model and simulation method are given in *SI Appendix*.

Data Availability. All of the data shown in the manuscript and *SI Appendix* have been deposited to Bitbucket (https://bitbucket.org/NUaztec/debarshee_trung_monica_pnas_2020/src/master/).

ACKNOWLEDGMENTS. This work was supported by the US Department of Commerce, National Institute of Standards and Technology as part of the Center for Hierarchical Materials Design under Award 70NANB19H005, and by the Sherman Fairchild Foundation. D.B. gratefully acknowledges fruitful discussions with F. Jiménez-Ángeles, and A. Ehlen for careful reading of the manuscript.

1. A. V. Dobrynin, M. Rubinstein, Theory of polyelectrolytes in solutions and at surfaces. *Prog. Polym. Sci.* **30**, 1049–1118 (2005).
2. M. Muthukumar, 50th anniversary perspective: A perspective on polyelectrolyte solutions. *Macromolecules* **50**, 9528–9560 (2017).
3. A. González, E. Goikolea, J. A. Barrena, R. Mysyk, Review on supercapacitors: Technologies and materials. *Renew. Sustain. Energy Rev.* **58**, 1189–1206 (2016).
4. L. Suo *et al.*, "Water-in-salt" electrolyte enables high-voltage aqueous lithium-ion chemistries. *Science* **350**, 938–943 (2015).
5. F. Jiménez-Ángeles, M. Lozada-Cassou, A model macroion solution next to a charged wall: Overcharging, charge reversal, and charge inversion by macroions. *J. Phys. Chem. B* **108**, 7286–7296 (2004).
6. T. Colla, M. Girotto, A. P. dos Santos, Y. Levin, Charge neutrality breakdown in confined aqueous electrolytes: Theory and simulation. *J. Chem. Phys.* **145**, 094704 (2016).
7. A. A. Lee, C. S. Perez-Martinez, A. M. Smith, S. Perkin, Scaling analysis of the screening length in concentrated electrolytes. *Phys. Rev. Lett.* **119**, 026002 (2017).
8. J. W. Zwanikken, M. Olvera de la Cruz, Tunable soft structure in charged fluids confined by dielectric interfaces. *Proc. Natl. Acad. Sci. U.S.A.* **110**, 5301–5308 (2013).
9. H. Li, A. Erbas, J. W. Zwanikken, M. Olvera de la Cruz, Ionic conductivity in polyelectrolyte hydrogels. *Macromolecules* **49**, 9239–9246 (2016).
10. O. A. Hickey, C. Holm, Electrophoretic mobility reversal of polyampholytes induced by strong electric fields or confinement. *J. Chem. Phys.* **138**, 194905 (2013).
11. B. Qiao, J. J. Cerda, C. Holm, Atomistic study of surface effects on polyelectrolyte adsorption: Case study of a poly (styrenesulfonate) monolayer. *Macromolecules* **44**, 1707–1718 (2011).
12. A. P. dos Santos, M. Girotto, Y. Levin, Simulations of polyelectrolyte adsorption to a dielectric like-charged surface. *J. Phys. Chem. B* **120**, 10387–10393 (2016).
13. Y. Jing, V. Jadhao, J. W. Zwanikken, M. Olvera de la Cruz, Ionic structure in liquids confined by dielectric interfaces. *J. Chem. Phys.* **143**, 194508 (2015).
14. A. P. dos Santos, Y. Levin, Electrolytes between dielectric charged surfaces: Simulations and theory. *J. Chem. Phys.* **142**, 194104 (2015).
15. J. Qin, Charge polarization near dielectric interfaces and the multiple-scattering formalism. *Soft Matter* **15**, 2125–2134 (2019).
16. R. Messina, Effect of image forces on polyelectrolyte adsorption at a charged surface. *Phys. Rev. E* **70**, 051802 (2004).
17. H. Wu, H. Li, F. J. Solis, M. Olvera de la Cruz, E. Luijten, Asymmetric electrolytes near structured dielectric interfaces. *J. Chem. Phys.* **149**, 164701 (2018).

18. S. K. Reed, O. J. Lanning, P. A. Madden, Electrochemical interface between an ionic liquid and a model metallic electrode. *J. Chem. Phys.* **126**, 084704 (2007).
19. M. K. Petersen, R. Kumar, H. S. White, G. A. Voth, A computationally efficient treatment of polarizable electrochemical cells held at a constant potential. *J. Phys. Chem. C* **116**, 4903–4912 (2012).
20. T. D. Nguyen, M. Olvera de la Cruz, Manipulation of confined polyelectrolyte conformations through dielectric mismatch. *ACS Nano* **13**, 9298–9305 (2019).
21. G. I. Guerrero-García, E. González-Tovar, M. Olvera de la Cruz, Effects of the ionic size-asymmetry around a charged nanoparticle: Unequal charge neutralization and electrostatic screening. *Soft Matter* **6**, 2056–2065 (2010).
22. L. Blum, J. L. Lebowitz, D. Henderson, A condition on the derivative of the potential in the primitive model of an electric double layer. *J. Chem. Phys.* **72**, 4249–4250 (1980).
23. D. T. Limmer *et al.*, Charge fluctuations in nanoscale capacitors. *Phys. Rev. Lett.* **111**, 106102 (2013).
24. P. Attard, D. Wei, G. N. Patey, On the existence of exact conditions in the theory of electrical double layers. *J. Chem. Phys.* **96**, 3767–3771 (1992).
25. G. M. Torrie, Negative differential capacities in electrical double layers. *J. Chem. Phys.* **96**, 3772–3774 (1992).
26. E. González-Tovar, F. Jiménez-Ángeles, R. Messina, M. Lozada-Cassou, A new correlation effect in the Helmholtz and surface potentials of the electrical double layer. *J. Chem. Phys.* **120**, 9782–9792 (2004).
27. M. B. Partenskii, V. Dorman, P. C. Jordan, The question of negative capacitance and its relation to instabilities and phase transitions at electrified interfaces. *Int. Rev. Phys. Chem.* **15**, 153–182 (1996).
28. M. B. Partenskii, P. C. Jordan, Limitations and strengths of uniformly charged double-layer theory: Physical significance of capacitance anomalies. *Phys. Rev. E* **77**, 061117 (2008).
29. M. J. Stevens, K. Kremer, Structure of salt-free linear polyelectrolytes. *Phys. Rev. Lett.* **71**, 2228–2231 (1993).
30. T. D. Nguyen, H. Li, D. Bagchi, F. J. Solis, M. Olvera de la Cruz, Incorporating surface polarization effects into large-scale coarse-grained molecular dynamics simulation. *Comput. Phys. Commun.* **241**, 80–91 (2019).
31. G. I. Guerrero-García, E. González-Tovar, M. Chávez-Páez, M. Lozada-Cassou, Overcharging and charge reversal in the electrical double layer around the point of zero charge. *J. Chem. Phys.* **132**, 054903 (2010).
32. R. Messina, E. González-Tovar, M. Lozada-Cassou, C. Holm, Overcharging: The crucial role of excluded volume. *Europhys. Lett.* **60**, 383–389 (2002).
33. J. A. C. Veerman, D. Frenkel, Phase behavior of disklike hard-core mesogens. *Phys. Rev. A* **45**, 5632–5648 (1992).
34. M. M. Hatlo, L. Lue, The role of image charges in the interactions between colloidal particles. *Soft Matter* **4**, 1582–1596 (2008).
35. Z. Wang, Y. Yang, D. L. Olmsted, M. Asta, B. B. Laird, Evaluation of the constant potential method in simulating electric double-layer capacitors. *J. Chem. Phys.* **141**, 184102 (2014).
36. Y. Matsumi, H. Nakano, H. Sato, Constant-potential molecular dynamics simulations on an electrode-electrolyte system: Calculation of static quantities and comparison of two polarizable metal electrode models. *Chem. Phys. Lett.* **681**, 80–85 (2017).
37. K. A. Dwelle, A. P. Willard, Constant potential, electrochemically active boundary conditions for electrochemical simulation. *J. Phys. Chem. C* **123**, 24095–24103 (2019).
38. V. Jadhao, F. J. Solis, M. Olvera de la Cruz, Simulation of charged systems in heterogeneous dielectric media via a true energy functional. *Phys. Rev. Lett.* **109**, 223905 (2012).
39. A. Campa, T. Dauxois, S. Ruffo, Statistical mechanics and dynamics of solvable models with long-range interactions. *Phys. Rep.* **480**, 57–159 (2009).